scientific reports

Check for updates

OPEN

An integrated multidimensional risk framework for volcanic hazard zones: insights from Mt. Vesuvius, Italy

Isabella Lapietra[1]✉, Federico Benassi[2], Thaís García-Pereiro[3], Anna Paterno[3] & Pierfrancesco Dellino[1]

Mt. Vesuvius, located in Campania Region (Southern Italy), is considered one of the world's most dangerous volcanoes due to its probability of future explosive eruptions in a densely populated area. When large populations or significant assets are exposed to volcanic hazards and exhibit high vulnerability, the potential for disaster increases. Consequently, combining volcanic hazard with demographic, social and building characteristics becomes essential to manage disasters. The approach presented in this work in based on integrated multidimensional and multisource framework aimed to risk analysis. It integrates diverse geospatial datasets, by exploring the relationship between long-term volcanic hazard (pyroclastic density currents), human population features (population exposure and social vulnerability) and building characteristics (building exposure and physical vulnerability). The challenge of this approach is to standardize the metrics belonging to physical hazard with those of potential vulnerability and exposure (which derived from different measures), to investigate the volcanic risk spatial distribution. By using Geographic Information System tools and statistical analyses, the approach identifies and prioritizes areas requiring focused mitigation strategies, at the Enumeration Area level. The resulting risk map highlights that areas classified as levels 4 and 5 are mainly concentrated in the northwestern sector of Mount Vesuvius, in particular inside the municipalities of Sant'Anastasia, Volla, Cercola, San Sebastiano al Vesuvio, Ercolano, Portici, and Naples.

Keywords Volcanic hazard, Exposure, Vulnerability, Statistical analysis, GIS

Cities located near volcanoes face direct and indirect threats from a range of volcanic hazards such as pyroclastic density currents (PDCs), lahars, lava flows, tephra and ash falls, gas, debris avalanches, landslides and, in case of proximity to the sea, tsunamis. All these natural hazards can potentially lead to loss of life and livelihoods, damage essential infrastructure, force population displacement and disrupt economic activities[1]. Currently, 500 million people globally live and work under the shadow of active volcanoes[2]although historically, severe urban settlements were affected by eruptions worldwide[3]. In this context, Mt. Vesuvius, in Campania Region (Southern Italy) (Fig. 1a), is widely recognized as one of the most dangerous for its probability of future explosive eruptions in a densely populated area[4–6]. In fact, more than 600,000 people live on the slopes of the volcano[7]. Historic and stratigraphic evidence of PDC and tephra fallout have underlined several eruptions in history[8]. The most famous and first documented Plinian eruption is the one that occurred on the 79 CE[9,10]that buried the cities of Pompeii, Oplontis, Stabies and Herculaneum, while the last eruption dates back to 1944[11]causing 14,000 people affected and 26 deaths[12]. The volcano is currently in a state of quiescence, marked solely by fumarolic activity and low seismicity[13], and it is continuously monitored by the surveillance network of the Vesuvius Observatory, the Naples branch of the Italian National Institute of Geophysics and Volcanology (INGV). In terms of risk management, the National Civil Protection Department (CPD), carries out activities of forecasting, prevention, and mitigation of volcanic risk in Italy and adopts measures aimed at reducing the loss of human lives and properties in the event of an eruption. The authority, that is also responsible for overseeing the phases of emergency management and recovery, with the efforts of the Campania Region, defined the National Emergency

[1]Department of Earth and Geoenvironmental Sciences, University of Bari "Aldo Moro", Bari 70125, Italy. [2]Department of Political Sciences, University of Naples Federico II, Naples 80133, Italy. [3]Department of Political Sciences, University of Bari "Aldo Moro", Bari 70125, Italy. ✉email: isabella.lapietra@uniba.it

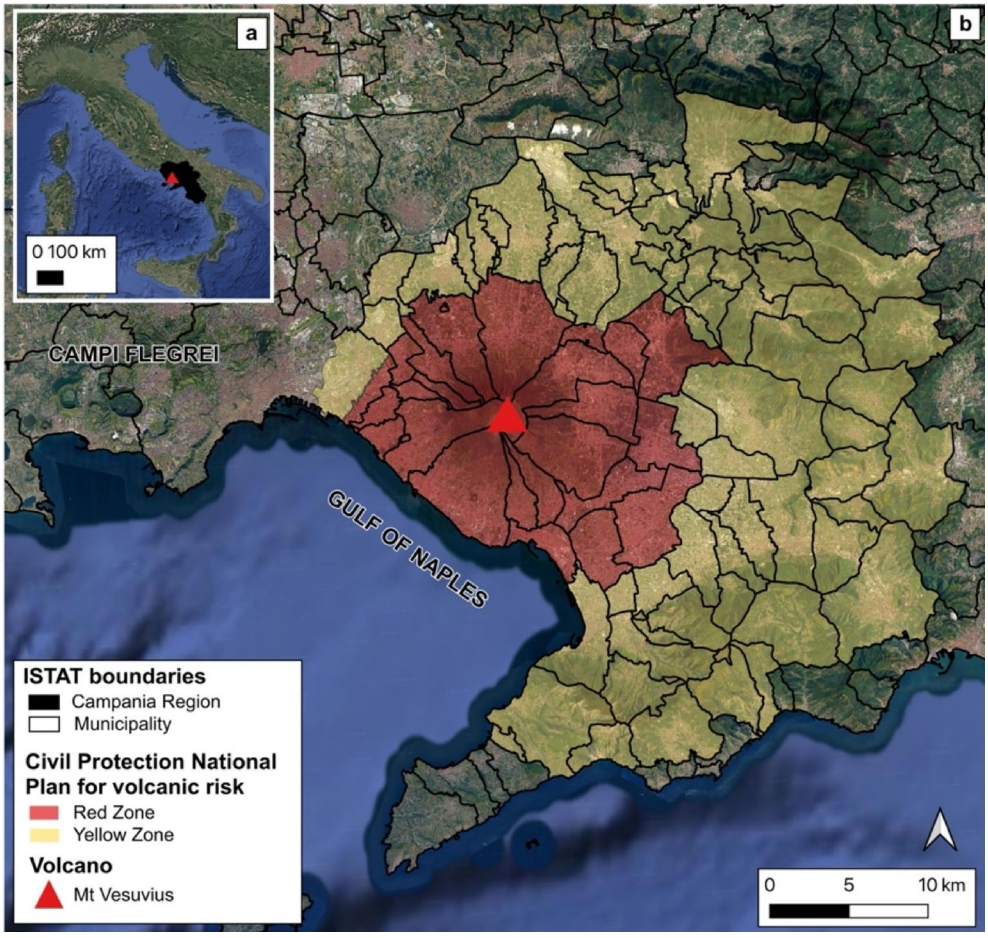

Fig. 1. Geographic setting of Mt. Vesuvius within the national context (**a**). Red and yellow zones included in the civil protection national plan of volcanic risk for the Vesuvius area[15] (**b**). The regional and municipality boundaries were retrieved from the Italian National Statistical Institute (ISTAT) dataset[16], while Google Satellite images were used as basemap. The figure was created in QGIS software 3.32.2.

Plans for the Vesuvius area individuating two zones (Fig. 1b): Red zone and Yellow zone. The Red one, covering 25 municipalities, includes the area exposed to pyroclastic flows (Red Zone 1) and the territory at high risk of roof collapse due to the accumulation of pyroclastic deposits (Red Zone 2). The Yellow zone, comprising of 63 municipalities and three districts of the City of Naples, represents the area exposed to significant fallout of volcanic ash and pyroclastic material. In this official document for emergency planning and evacuation for the Vesuvius area, the Red zone map identifies the areas potentially exposed to PDCs but does not take into account the impact that PDCs could have on buildings and people. For this purpose, it should be requested the distribution of the impact parameters related to PDCs (e.g. flow temperature, flow duration, particle concentration and flow dynamic pressure) that better represent flow intensity in terms of damage potential over the volcano's surroundings[14].

For this reason and knowing that disaster risk depends on the severity of hazard, the number of people or assets exposed and the vulnerability or susceptibility of these elements to suffer loss and damage[17], combining volcanic hazard with demographic, social and building characteristics is crucial to manage disaster risk in highly populated areas such as the Mt. Vesuvius. The present research applies an integrated multidimensional and multisource framework for disaster risk analysis based upon the definition provided by the United Nations Office for Disaster Risk Reduction (UNDRR)[17]. The approach explores the relationship between the following dimensions: long-term volcanic hazard (pyroclastic density currents, PDCs), human population features (population exposure and social vulnerability) and building characteristics (building exposure and physical vulnerability). Volcanic hazard can be defined as the probability of long-term occurrence of PDCs to damage a territory in a specified period of time that is useful for cost/benefit analysis of risk mitigation actions[18], and for appropriate land use planning and location of settlements. Population and building exposure represent the number of people and buildings exposed to long-term volcanic hazard; while social and physical vulnerability can be described as the combination of demographic, socioeconomic factors and building characteristics that can (potentially) increase the impacts of the element exposed[19]. Over the past two decades, several studies have attempted to integrate hazard, exposure, and vulnerability in volcanic settings worldwide[20–28]. In the Vesuvius area, however, research mainly addressed one or two components of risk such as exposure and hazard[29]; building

exposure and physical vulnerability[30–32]; overall vulnerability[33]; population exposure and social vulnerability[34]; hazard assessment[14,18,35,36]; or focusing on risk perception[37–39]. A further challenge lies in conducting risk analyses at the local level, where the lack of high-resolution spatial demographic and socio-economic census data[40]hampers comprehensive planning and necessitates spatial assessments that integrate place-specific hazard characteristics with demographic, social, and economic conditions at the Enumeration Area (EA) scale[41]. These aspects underlined the need to build a new approach that covers all the not previously examined aspects of risk through a multidisciplinary lens at the local level.

The main aims are the investigation and mapping of (i) volcanic hazard, (ii) exposure, (iii) vulnerability and (iv) volcanic risk in the Mt. Vesuvius area at EA level in order to gain information about (v) inhabitants and buildings located within the different risk levels for cost-benefit analysis, land-use planning, risk mitigation, disaster preparedness, and community resilience. The challenge of this approach is to standardize the metrics belonging to physical hazard with those of vulnerability and exposure (which derived from different measures and sources) and to quantify volcanic risk. The study presents a clear and simplified methodological procedure based on diverse integrated geospatial datasets. The main results are presented in form of maps, while tables, included as supplementary materials, are provided to show the level of hazard, exposure, vulnerability and risk in each municipality under investigation.

Results

Volcanic hazard

The spatial distribution of the volcanic hazard index (see Methods section) identifies an area of 432 km^2 (Fig. 2a) which includes 43 municipalities and 6,608 EAs (Fig. S1 – supplementary) with a total population of 1,075,508 inhabitants and 100,804 buildings (Tab.S1 - supplementary). Figure 2b shows the volcanic hazard level distribution across the EAs under investigations. Level 1 corresponds to very low hazard, 2 to low hazard, 3 to medium hazard, 4 to high hazard and 5 to very high hazard (see Methods section). The map highlights that the highest hazard levels (4 and 5) occur in EAs located near the volcano, particularly within municipalities of Sant'Anastasia, Pollena Trocchia, Somma Vesuviana, Ottaviano, and Massa di Somma with level 5 extending in the northwestern direction. Hazard levels gradually decrease with increasing distance from the volcano, reaching the lowest levels (1 and 2) near the outer boundaries of the study area. Consequently, municipalities that extend from the slopes of Mt. Vesuvius down to lower-altitude coastal zones — including Napoli, Ercolano, and Torre del Greco — may encompass the full range of volcanic hazard levels. Tab. S2 (supplementary) summarizes the distribution of EA hazard levels across the municipalities under investigation.

Exposure

Figure 3 illustrates the spatial distribution of population density (Fig. 3a), building density (Fig. 3b), and the overall exposure (Fig. 3c). Exposure levels are classified from 1 (very low) to 5 (very high) (see Methods section).

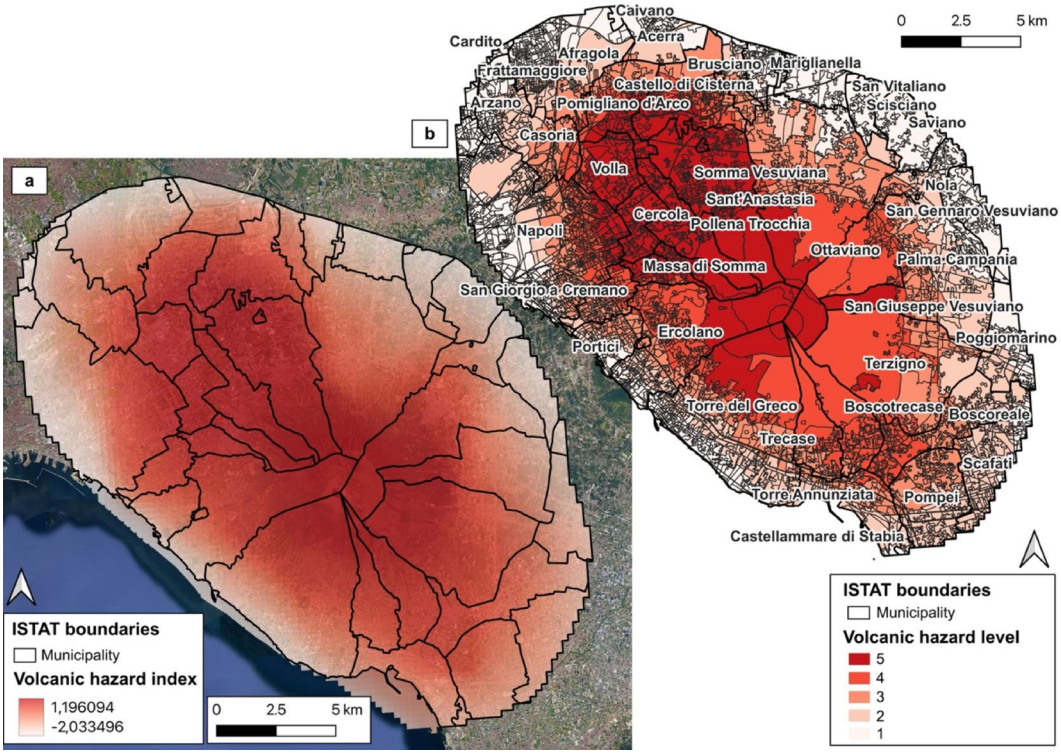

Fig. 2. Spatial distribution of volcanic hazard index at grid scale (**a**) and volcanic hazard level at EA scale (**b**). Google Satellite was used as a basemap (**a**) and the figures were generated in QGIS software 3.32.2.

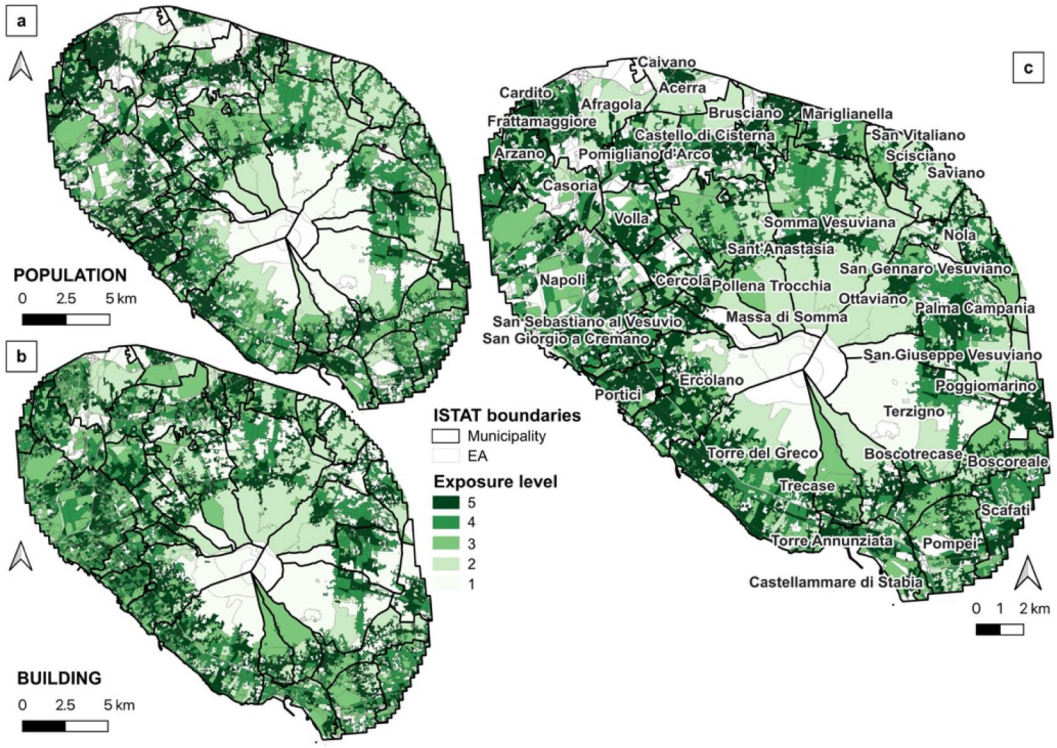

Fig. 3. Spatial distribution of population (**a**), building (**b**) and overall (**c**) exposure at EA scale. The figures were generated in QGIS software 3.32.2.

As observed in the maps, the lowest exposure levels (1 and 2) are predominantly found in EAs located near the volcano and, more generally, in the northeastern portion of the study area. In contrast, exposure hotspots, characterized by levels 4 and 5, are primarily clustered within coastal municipalities such as Portici, San Giorgio a Cremano, Napoli, and Ercolano, as well as in the western sector of the study area. Tab. S3 (supplementary) summarizes the distribution of exposure levels across the municipalities under investigation.

Vulnerability

Figure 4 depicts the spatial distribution of social (Fig. 4a), physical (Fig. 4b), and overall (Fig. 4c) vulnerability levels (see Methods section). The classification scheme ranges from 1 (very low vulnerability) to 5 (very high vulnerability). As shown in the maps, the lowest vulnerability levels (1 and 2) are predominantly found in EAs located in the southeastern portion of the study area, particularly within the municipalities of Scafati, Terzigno, Pompei, and Palma Campania. Conversely, EAs located in the western sector of the volcanic area exhibit higher vulnerability levels (3, 4, and 5), notably within the municipalities of Sant'Anastasia, Volla, Portici, and Afragola. Consistently with the other risk components, Tab. S4 (supplementary) shows the distribution of overall vulnerability levels across the municipalities under investigation.

Volcanic risk

Figure 5 shows the final results derived from the integration of volcanic hazard, exposure, and vulnerability layers (see Methods section), depicting the spatial distribution of volcanic risk levels across the examined EAs. The classification ranges from 1 (very low volcanic risk) to 5 (very high volcanic risk). Overall, the map reveals that EAs characterized by the highest risk levels (4 and 5), shown in orange and in red, are mainly concentrated in the northwestern portion of the study area—particularly within the municipalities of Sant'Anastasia, Volla, Cercola, San Sebastiano al Vesuvio, and along the coastal municipalities of Ercolano, Portici, and Napoli. Conversely, lower risk levels are primarily distributed around the volcano and throughout the eastern sectors of the study area. As reported in Tab. S5 (supplementary), half of the municipalities under investigation are characterized by high and very high volcanic risk levels (levels 4 and 5) while Fig.S2 (supplementary) shows the proportion of inhabitants (Fig. S2a) and buildings (Fig. S2b) located within each volcanic risk level in the analyzed municipalities.

At the scale of the entire study area, 88.86% of the population resides within EAs exposed to volcanic risk, distributed as follows: 4.45% at very low risk, 9.97% at low risk, 14.35% at medium risk, 23.14% at high risk, and 36.94% at very high risk. Regarding buildings, 92.42% are located within areas exposed to volcanic risk: 7.62% at very low risk, 11.63% at low risk, 23.23% at medium risk, 20.70% at high risk, and 29.24% at very high risk.

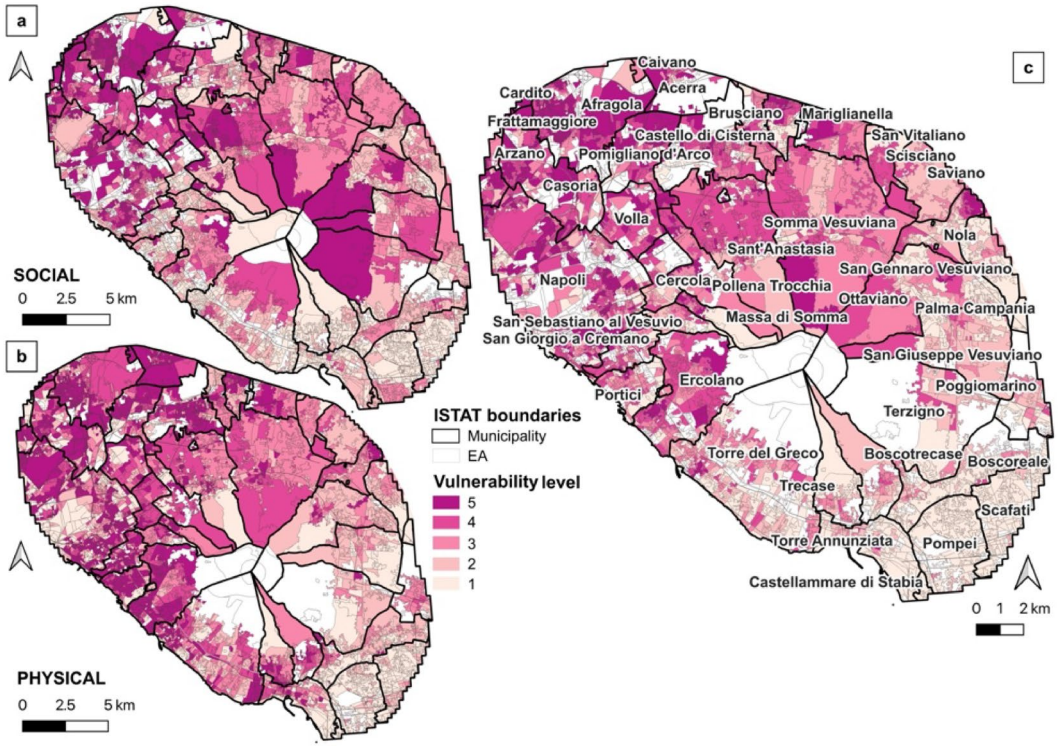

Fig. 4. Spatial distribution of social (**a**), physical (**b**) and overall (**c**) vulnerability at EA scale. The figures were generated in QGIS software 3.32.2.

Discussion

The integrated multidimensional framework underscores four key aspects in disaster studies: the need of robust risk quantification, the importance of representing the risk spatial distribution, the development of spatially targeted mitigation strategies and the significance of data in high-resolution risk assessment.

Risk calculation, based on the combined investigation of hazard, exposure, and vulnerability, aligns with recent international frameworks[17,42,43]and serves as an effective interface between scientific research and policy-making[44]. The use of composite risk indices enables systematic comparisons across regions, spatial scales, and time periods[45,46]supporting the development of future scenarios, and facilitating mitigation planning and emergency management under conditions of uncertainty. Although disasters are inherently unpredictable, methodologies that identify populations and assets within the highest risk classes (Fig. S2 -supplementary) can substantially reduce loss of life, physical damage, and emergency-related costs[43,47].

Risk mapping allows for the identification of the components that most strongly influences the overall risk, thereby improving the understanding of the main risk drivers. For instance, in the municipality of Ercolano (Fig. S3 – supplementary), volcanic risk patterns are largely shaped by vulnerability, whereby the overall risk level is mainly determined by hazard and exposure. This highlights the context-specific nature of risk, whereby certain components exert a greater influence on risk than others[40]. As a consequence, comparing Fig. 5 with Fig. 1c, this framework achieves a more detailed risk classification—five levels instead of two - enabling spatially targeted mitigation strategies, more accurate estimation of populations requiring evacuation and reducing emergency management costs.

Given that most mitigation strategies in volcanic hazard zones are primarily grounded on hazard assessment alone[15,48,49], the present approach could offer two alternative perspectives for designing mitigation measures: (a) mitigation targeting the component with the major influence on overall risk, and (b) mitigation differentiated by levels of risk. Considering the municipality of Ercolano (Fig. S3 - supplementary), the first approach (a) could focus on reducing vulnerability. With this regard, both social and physical vulnerability maps (Fig. 4a and b) may be employed to identify and prioritize mitigation actions based on specific vulnerability levels[50–52], taking into account social factors and structural reinforcement of the built environment. In municipalities where hazard or exposure represents risk drivers, targeted mitigation strategies could be focused on early-warning and monitoring systems or on urban planning and relocation. The second approach (b) would enable the definition of mitigation measures that progressively intensify, from risk level 1 to level 5. Under this perspective, level 1 areas would primarily involve maintaining public awareness and readiness without requiring direct interventions; level 2 areas would involve restrictions on new developments and the planning of simple evacuation routes and communication systems; level 3 areas would focus on enhancing preparedness through community training and improved monitoring and early-warning systems; level 4 areas would require continuous monitoring, enforcement of restricted zones, and optimized evacuation logistics; and level 5 areas would demand comprehensive protective strategies aimed at safeguarding human life and ensuring rapid

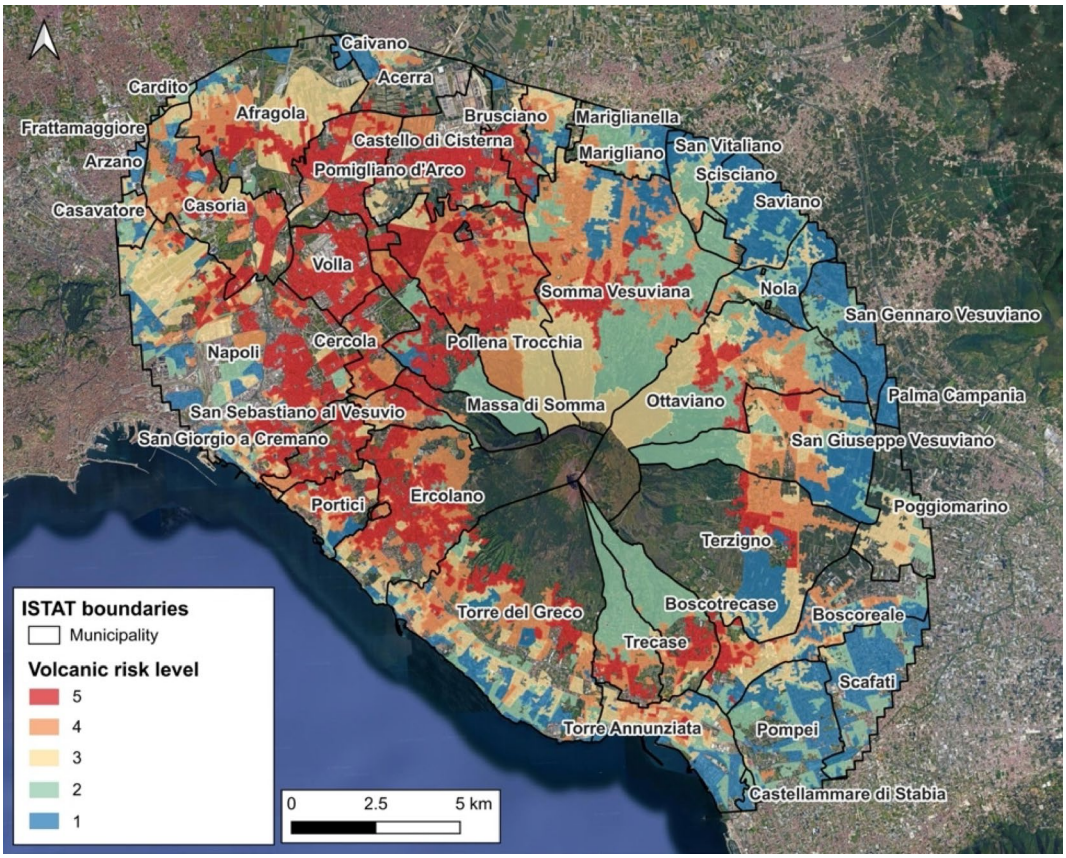

Fig. 5. Spatial distribution of volcanic risk levels at EA scale. Google Satellite image was used as a basemap and the entire figure was generated in QGIS software 3.32.2. The map highlights only the EAs included in the different volcanic risk levels.

recovery. In this context, Fig. 5 and Fig.S2 (supplementary) could represent the base of this approach in terms of critical areas and number of inhabitants and buildings at volcanic risk.

The extrapolation of volcanic risk data at the municipal scale can serve as a fundamental basis for damage assessment, decision-making processes, cost–benefit analyses[53,54], and for the activities of insurance companies[55,56].

Although the proposed methodology underscores the value of risk quantification, two main limitations should be acknowledged. The unavailability of more recent census variables at the sub-municipal scale, especially for building-related information - that allowed us to use the 2011 dataset (Tab.S6-supplementary)— constrains the accuracy of the recent characteristics of the built environment, thus restricting the overall precision of vulnerability assessments. Consequently, improving socio-economic data collection at finer spatial resolutions is essential to support more robust and statistically rigorous risk analyses. Lastly, the uncertainty quantification is essential to improve the validity of risk assessment and could represent the development of the present research[57,58].

Despite some limitations, the findings obtained by the present approach could contributes to the construction of a comprehensive geospatial database for the Mt. Vesuvius area, associating each EA with corresponding levels of hazard, exposure, vulnerability, and risk. Such a database could be updated on an annual basis, representing a practical tool for stakeholders and local authorities. The proposed methodology, which integrates statistical analyses and cartographic data, enables the synthesis of diverse metrics within a coherent analytical framework that is applicable not only to volcanic contexts but also to other natural hazards and socio-demographic profiles. It may further serve as a foundation for developing a multi-hazard framework within the same territorial context especially in the Mt. Vesuvius area which is located within a complex volcanic system that includes Campi Flegrei and Ischia Island, supporting long-term and multi-risk mitigation planning.

Methods

The integrated multidimensional framework

According to UNDRR[16], the framework was based on the risk formula expressed through Eq. (1):

$$VR = VH * E * V \tag{1}$$

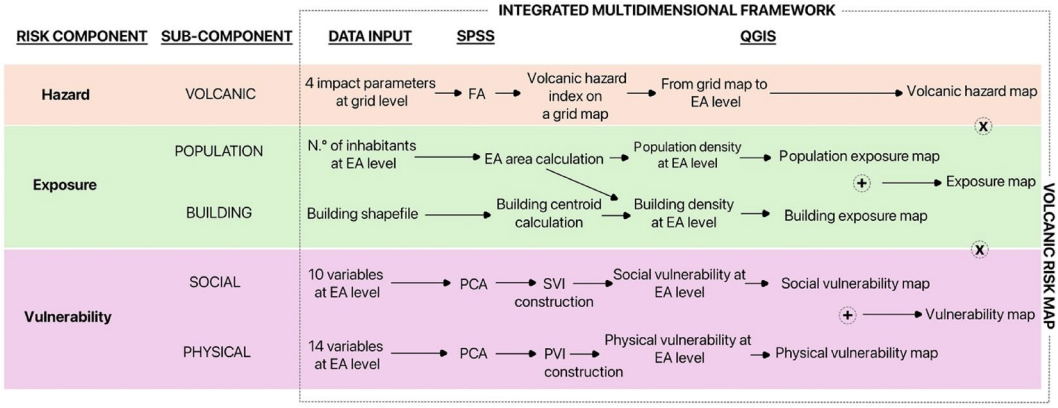

Fig. 6. Operational workflow for volcanic risk analysis. For *DATA INPUT* please refers to Table S6 (Supplementary). Symbol + represents a sum, while symbol x represents a multiplication.

Where volcanic risk (VR) is described as a multidimensional entity deriving from the product of three dimensions: volcanic hazard (VH), exposure (E), and vulnerability (V). The equation enables quantitative risk assessment through the integration of heterogeneous data belonging to different components (H, E, V). The aggregation of multiple variables linked to these components, can be supported by the construction of synthetic indexes that can be mapped and combined for risk calculation[40]. Particularly, multivariate statistical analyses such as Factor Analysis (FA) or Principal Component Analysis (PCA) are commonly used for hazard and social vulnerability index construction[59–62]while GIS tools are generally implemented to represent the spatial distribution of these indexes[63,64]. GIS and statistical analyses were performed for index construction, level classification, mapping and data layers integration at EA scale. The operational workflow (Fig. 6) was carried out by the use of Statistical Package for the Social Sciences (SPSS) and QGIS software. A multi-source approach was adopted to collect volcanic hazard, building exposure, population characteristics and building structural conditions. These variables are summarized and described in detail in Tab. S6 (supplementary).

Long-term volcanic hazard was expressed in terms of four pyroclastic density current (PDC) impact parameters (Table S6-supplementary) which represent key PDC flow properties relevant for evaluating the potential damage[14]and constructing the volcanic hazard index. These variables, that were originally mapped on a regular grid (cell = 250*250m)[14], were first standardized in SPSS to make them comparable. Then, the main factor, extracted from the FA computed in the same software, was used to map the volcanic hazard index (Fig. 2a). The overlay between the volcanic hazard index map (Fig. 2a) with the 2021 ISTAT boundaries[16]allowed for the study area selection (Fig. S1 – supplementary) and the volcanic hazard cell values were transferred from the grid to EA scale following the approach provided by Pratschke & Benassi[65]. The resulting vector dataset was converted into raster format and linearly rescaled into five levels ranging from 1 (very low hazard) to 5 (very high hazard) (Fig. 2b). Rescaling preserves spatial relationships while standardizing the index for comparison and integration with other risk components.

Following the approach proposed by Lapietra et al.[40], the exposure index, was constructed in QGIS with the use of the number of inhabitants and buildings located in possibly affected EAs (Table 6 – supplementary). As concerns the population exposure, the population density of each EA was calculated as a ratio between the number of inhabitants and the total extent of the EA. For building density, building centroids were extracted in QGIS from the CPD structural aggregates shapefile (Table 6 – supplementary) to count the number of buildings within each EA. The resulting values were then normalized by EAs area to calculate building density. The resulting vector layers (population density and building density) were converted into raster and rescaled from 1 (very low exposure) to 5 (very high exposure) (Fig. 3a and 3b). Using the QGIS Raster Calculator, total exposure was obtained by summing the population and building exposure that was successively rescaled into five levels from 1 (very low exposure) to 5 (very high exposure) (Fig. 3c). EAs with zero population and buildings were excluded from the analysis.

The vulnerability index was expressed in terms of social and physical dimensions. Eight variables, describing the demographic and socioeconomic conditions at the EA level were used to investigate social vulnerability (Table 6 - supplementary). While, physical vulnerability was evaluated by the use of ten variables representing the structural and housing characteristics (Tab. S6 – supplementary). Since the absence of standardized guidelines for vulnerability index construction[64], the variable selection was guided by consistency with recent literature[40,64,66] and data availability at the EA scale[16,67]. In addition, the selected variables (Table 6 – supplementary), also included spatial features of each EA expressed through centroid coordinates[68,69]. All data were standardized and analyzed in SPSS. A first PCA was performed to synthetize ten variables into three factors that mainly influenced the social vulnerability dataset. The composite Social Vulnerability Index (SVI) was then calculated for each EA using Eq. (2) proposed by Siagian et al.[70]:

$$SVI = \frac{\sum_{i=1}^{N}(F_i * V_i)}{V_{tot}} \quad (2)$$

where F_i represents factor i; V_i is the variance of F_i; V_{tot} is the total variance and N the total number of factors. The results were mapped, converted into raster, and rescaled from 1 (very low social vulnerability) to 5 (very high social vulnerability) (Fig. 4a). Physical vulnerability was evaluated using the same statistical procedure and the same index construction (Eq. 2). However, since building data referred to 2011 ISTAT boundaries (Tab. S6 - Supplementary), the physical vulnerability cell values were transferred from 2011 EA to 2021 EA scale using QGIS[65]. The resulting vector dataset was converted into raster format and rescaled from 1 (very low physical vulnerability) to 5 (very high physical vulnerability) (Fig. 4b). Following Fig. 6, the overall vulnerability was obtained by summing the social and physical vulnerability raster using the QGIS Raster Calculator and the resulting layer was rescaled from 1 to 5 (Fig. 4c) to ensure consistency with the hazard and exposure components.

Lastly, according to Eq. (1), volcanic risk was estimated by multiplying hazard, total exposure, and overall vulnerability layers using the QGIS raster calculator tool. The resulting risk raster was classified using a quantile-based approach into very low (1), low (2), medium (3), high (4), and very high (5) volcanic risk levels (Fig. 5). This classification enabled the quantification of both population and buildings within each volcanic risk class (Fig. S2 - supplementary).

Data availability

Data will be made available on request by contacting the following email address: isabella.lapietra@uniba.it.

Received: 18 November 2025; Accepted: 13 February 2026
Published online: 20 February 2026

References

1. Loughlin, S. C., Sparks, R. S. J., Brown, S. K., Jenkins, S. F. & Vye-Brown, C. *Global volcanic hazards and risk*. https://www.cambridge.org/core/services/aop-cambridge-core/content/view/7653B9CA75E2F32A81CE5B7110BEF8AB/9781107111752AR.pdf/Global_Volcanic_Hazards_and_Risk.pdf?event-type=FTLA (Cambridge University Press, 2015).
2. Freire, S., Florczyk, A. J., Pesaresi, M. & Sliuzas, R. An improved global analysis of population distribution in proximity to active volcanoes, 1975–2015. *ISPRS Int. J. Geo-Inf.* **8** (8), 341. https://doi.org/10.3390/ijgi8080341 (2019).
3. Meredith, E. S. et al. Cities near volcanoes: which cities are most exposed to volcanic hazards? *NHESS*, 1–36 https://doi.org/10.5194/nhess-25-2731-2025 (2025).
4. Gurioli, L. et al. Pyroclastic flow hazard assessment at Somma-Vesuvius based on the geological record. *Bull. Volcanol.* **72**, 1021–1038. https://doi.org/10.1007/s00445-010-0379-2 (2010).
5. Lirer, L., Petrosino, P. & Alberico, I. Hazard and risk assessment in a complex multi-source volcanic area: the example of the campania Region, Italy. *Bull. Vulcanol.* **72** (4), 411–429. https://doi.org/10.1007/s00445-009-0334-2 (2010).
6. Baxter, P. J. et al. Emergency planning and mitigation at vesuvius: A new evidence-based approach. *J. Volcanol Geotherm.* **178** (3), 454–473. https://doi.org/10.1016/j.jvolgeores.2008.08.015 (2008).
7. Civil Protection Department. Risks. https://rischi.protezionecivile.gov.it/en/volcanic/volcanoes-italy/vesuvio/
8. INGV. Osservatorio Vesuviano, Sezione di Napoli. https://www.ov.ingv.it/index.php/storia-vesuvio
9. Dellino, P., Dioguardi, F., Isaia, R., Sulpizio, R. & Mele, D. The impact of pyroclastic density currents duration on humans: the case of the AD 79 eruption of vesuvius. *Sci. Rep.* **11**, 4959. https://doi.org/10.1038/s41598-021-84456-7 (2021).
10. Doronzo, D. M. et al. The 79 CE eruption of vesuvius: A lesson from the past and the need of a multidisciplinary approach for developments in volcanology. *Earth Sci. Rev.* **231**, 104072. https://doi.org/10.1016/j.earscirev.2022.104072 (2022).
11. Cubellis, E., Marturano, A. & Pappalardo, L. The last vesuvius eruption in March 1944: reconstruction of the eruptive dynamic and its impact on the environment and people through witness reports and volcanological evidence. *Nat. Hazards*. **82**, 95–121. https://doi.org/10.1007/s11069-016-2182-7 (2016).
12. EM-DAT dataset. https://public.emdat.be/data
13. Rosi, M., Acocella, V., Cioni, R., Bianco, F., Costa, A., De Martino, P., Inguaggiato,S. Defining the pre-eruptive states of active volcanoes for improving eruption forecasting. *Front. Earth Sci.* **10**, 795700 (2022).
14. Dellino, P., Dioguardi, F., Sulpizio, R. & Mele, D. Long-term hazard of pyroclastic density currents at vesuvius (Southern Italy) with maps of impact parameters. *Nat. Hazards Earth Syst. Sci.* **25**, 2823–2844. https://doi.org/10.5194/nhess-25-2823-2025 (2025).
15. Civil Protection Department. Piano nazionale di protezione civile per il rischio vulcanico al Vesuvio. https://www.protezionecivile.gov.it/it/approfondimento/aggiornamento-del-piano-nazionale-di-protezione-civile-il-vesuvio/
16. ISTAT. Basi territoriali e variabili censuarie dataset. https://www.istat.it/notizia/basi-territoriali-e-variabili-censuarie/
17. UNDRR. *Global Assessment Report on Disaster Risk Reduction 2022: our World at Risk: Transforming Governance for a Resilient Future* https://www.undrr.org/gar/gar2022-our-world-risk-gar (United Nations Office for Disaster Risk Reduction, 2022).
18. Marzocchi, W., Sandri, L., Gasparini, P., Newhall, C. & Boschi, E. Quantifying probabilities of volcanic events: the example of volcanic hazard at Mount vesuvius. *J. Geophys. Res: Solid Earth*. **109** (B11). https://doi.org/10.1029/2004JB003155 (2004).
19. Birkmann, J., Sorg, L. & Welle, T. Disaster vulnerability. In The Palgrave Handbook of Unconventional Risk Transfer, 329–356 (Springer International Publishing, 2017).
20. Córdoba, G. A. et al. Assessing probabilistic hazard and risk for building, road network, and ecosystems: the case study of La Florida municipality, Galeras Volcano, Colombia. *Front. Earth Sci.* **13**, 1632282. https://doi.org/10.3389/feart.2025.1632282 (2025).
21. Sparks, R. S. J. et al. Future eruptions of the Kolumbo volcanic field: prognosis with hazard and risk assessment. *Bull. Volc.* **87** (9), 1–29. https://doi.org/10.1007/s00445-025-01836-x (2025).
22. Muryani, C., Noviani, R. & Azizah, R. N. Disaster risk analysis of Merapi Volcano eruption in the north slope based on the New Volcanic Risk Ranking (VRR) methods. *IOP Conf. Ser.: Earth Environ. Sci.* **1314** (1), 012015 https://doi.org/10.1088/1755-1315/1314/1/012015 (IOP Publishing, 2024).
23. Nieto-Torres, A., Del Pozzo, A. L. M., Groppelli, G. & Viera, M. D. C. J. Risk scenarios for a future eruption in the Chichinautzin monogenetic volcanic field, South México City. *J. Volcanol Geotherm.* **433**, 107733. https://doi.org/10.1016/j.jvolgeores.2022.107733 (2023).
24. Nieto-Torres, A., Guimarães, L. F., Bonadonna, C. & Frischknecht, C. A new inclusive volcanic risk ranking, part 1: methodology. *Front. Earth Sci.* **9**, 697451. https://doi.org/10.3389/feart.2021.697451 (2021).
25. Bonadonna, C. et al. Integrating hazard, exposure, vulnerability and resilience for risk and emergency management in a volcanic context: the ADVISE model. *J. Appl. Volcanol.* **10** (1), 7. https://doi.org/10.1186/s13617-021-00108-5 (2021).
26. Guimarães, L. F., Nieto-Torres, A., Bonadonna, C. & Frischknecht, C. A new inclusive volcanic risk ranking, part 2: application to Latin America. *Front. Earth Sci.* **9**, 757742. https://doi.org/10.3389/feart.2021.757742 (2021).

27. Reyes-Hardy, M. P., Barraza, F. A., Birke, J. P. S., Cáceres, A. E. & Pizarro, M. I. GIS-based volcanic hazards, vulnerability and risks assessment of the guallatiri Volcano, Arica y Parinacota Region, Chile. *J. South. Am. Earth Sci.* **109**, 103262. https://doi.org/10.1016/j.jsames.2021.103262 (2021).
28. Jumadi, J., Malleson, N., Carver, S. & Quincey, D. Estimating spatio-temporal risks from volcanic eruptions using an agent-based model. *JASSS* **23** (2), https://doi.org/10.18564/jasss.4241 (2020).
29. Alberico, I., Petrosino, P. & Lirer, L. Volcanic hazard and risk assessment in a multi-source volcanic area: the example of Napoli City (Southern Italy). *NHESS* **11** (4), 1057–1070. https://doi.org/10.5194/nhess-11-1057-2011 (2011).
30. Zuccaro, G. & De Gregorio, D. Impact assessments in volcanic areas-The vesuvius and Campi flegrei cases studies. *Ann. Geophys.* **62** (1), VO02–VO02. https://doi.org/10.4401/ag-7827 (2019).
31. Zuccaro, G. & De Gregorio, D. Time and space dependency in impact damage evaluation of a sub-Plinian eruption at Mount vesuvius. *Nat. Hazards.* **68** (3), 1399–1423. https://doi.org/10.1007/s11069-013-0571-8 (2013).
32. Spence, R. J., Baxter, P. J. & Zuccaro, G. Building vulnerability and human casualty Estimation for a pyroclastic flow: a model and its application to vesuvius. *J. Volcanol geotherm.* **133** (1–4), 321–343. https://doi.org/10.1016/S0377-0273(03)00405-0 (2004).
33. Willis, I., Gibin, M., Barros, J. & Webber, R. Applying neighbourhood classification systems to natural hazards: a case study of Mt vesuvius. *Nat. Hazards.* **70** (1), 1–22. https://doi.org/10.1007/s11069-010-9648-9 (2014).
34. Pesaresi, C., Marta, M., Palagiano, C. & Scandone, R. The evaluation of social risk due to volcanic eruptions of vesuvius. *Nat. Hazards.* **47** (2), 229–243. https://doi.org/10.1007/s11069-008-9214-x (2008).
35. Sulpizio, R., Folch, A., Costa, A., Scaini, C. & Dellino, P. Hazard assessment of far-range volcanic Ash dispersal from a violent strombolian eruption at Somma-Vesuvius volcano, Naples, italy: implications on civil aviation. *Bull. Volcanol.* **74** (9), 2205–2218. https://doi.org/10.1007/s00445-012-0656-3 (2012).
36. Rolandi, G. Volcanic hazard at vesuvius: an analysis for the revision of the current emergency plan. *J. Volcanol geotherm.* **189** (3–4), 347–362. https://doi.org/10.1016/j.jvolgeores.2009.08.007 (2010).
37. Avvisati, G. et al. Perception of risk for natural hazards in campania region (Southern Italy). *IJDRR* **40**, 101164. https://doi.org/10.1016/j.ijdrr.2019.101164 (2019).
38. Ricci, T., Nave, R. & Barberi, F. Vesuvio civil protection exercise MESIMEX: survey on volcanic risk perception. *Ann. Geophys.* **56** (4), S0452–S0452. https://doi.org/10.4401/ag-6458 (2013).
39. Carlino, S., Somma, R. & Mayberry, G. C. Volcanic risk perception of young people in the urban areas of vesuvius: comparisons with other volcanic areas and implications for emergency management. *J. Volcanol geotherm.* **172** (3–4), 229–243. https://doi.org/10.1016/j.jvolgeores.2007.12.010 (2008).
40. Lapietra, I., Benassi, F., Paterno, A., García-Pereiro, T. & Dellino, P. Mapping social risk areas to floods in Southern italy: a Spatial analysis for local emergency planning and place-based risk reduction policies. *IJDRR* 105666. https://doi.org/10.1016/j.ijdrr.2025.105666 (2025).
41. Buck, K. D. & Summers, J. K. Application of a multi-hazard risk assessment for local planning. *Geomatics Nat. Hazards Risk.* **11** (1), 2058–2078 (2020). https://doi.org/10.1080/19475705.2020.1828190.
42. UNISDR. Sendai Framework for Disaster Risk Reduction 2015–2030 (p. 32). United Nations Office for Disaster Risk Reduction (UNISDR). https://www.undrr.org/media/16176/download?startDownload=20260204
43. Field, I. P. C. C. et al. The Edinburgh Building, Shaftesbury Road, Cambridge CB2 8RU ENGLAND, pp. 582, (Cambridge University Press, 2012).
44. Kelman, I. Climate change and the Sendai framework for disaster risk reduction. *Int. J. Disaster Risk Sci.* **6**, 117–127. https://doi.org/10.1007/s13753-015-0046-5 (2015).
45. Garschagen, M., Doshi, D., Reith, J. & Hagenlocher, M. Global patterns of disaster and climate risk-an analysis of the consistency of leading index-based assessments and their results. *Clim. Change.* **169** (1), 11. https://doi.org/10.1007/s10584-021-03209-7 (2021).
46. Ward, P. J. et al. Natural hazard risk assessments at the global scale. *NHESS* **20** (4), 1069–1096. https://doi.org/10.5194/nhess-20-1069-2020 (2020).
47. Badreldin, H., Scaini, C., Hassan, H. M. & Peresan, A. High-resolution multi-hazard residential buildings and population exposure model for coastal areas: A case study in northeastern Italy. *IJDRR* 121, 105403 https://doi.org/10.1016/j.ijdrr.2025.105403 (2025).
48. Marrero, J. M. et al. Strategies for the development of volcanic hazard maps in monogenetic volcanic fields: the example of La Palma (Canary Islands). J. *Appl. Volcanol* 8 (1), 1–21 (2019).
49. Takarada, S. The volcanic hazards assessment support system for the online hazard assessment and risk mitigation of quaternary volcanoes in the world. *Front. Earth Sci.* **5**, 102. https://doi.org/10.3389/feart.2017.00102 (2017).
50. Sapountzaki, K. Risk mitigation, vulnerability management, and resilience under disasters. *Sustainability* **14** (6), 3589. https://doi.org/10.3390/su14063589 (2022).
51. Frigerio, I. & De Amicis, M. Mapping social vulnerability to natural hazards in italy: A suitable tool for risk mitigation strategies. *Environ. Sci. Policy.* **63**, 187–196. https://doi.org/10.1016/j.envsci.2016.06.001 (2016).
52. Menoni, S., Molinari, D., Parker, D., Ballio, F. & Tapsell, S. Assessing multifaceted vulnerability and resilience in order to design risk-mitigation strategies. *Nat. Hazards.* **64** (3), 2057–2082. https://doi.org/10.1007/s11069-012-0134-4 (2012).
53. Woo, G. Cost–benefit analysis in volcanic risk. In *Volcanic hazards, risks and disasters*, 289–300 https://doi.org/10.1016/B978-0-12-396453-3.00011-3 (Elsevier, 2015).
54. Sandri, L., Jolly, G., Lindsay, J., Howe, T. & Marzocchi, W. Combining long-and short-term probabilistic volcanic hazard assessment with cost-benefit analysis to support decision making in a volcanic crisis from the Auckland volcanic Field, new Zealand. *Bull. Volcanol.* **74** (3), 705–723. https://doi.org/10.1007/s00445-011-0556-y (2012).
55. Kalfin, K., Sukono, S., Januaviani, T. M. A. & Siregar, B. Determination of Mount eruption insurance premiums in Indonesia based on collective risk and level of risk spread. *IJBESD* **5** (1), 38–44. https://doi.org/10.46336/ijbesd.v5i1.576 (2024).
56. Smolka, A. & Käser, M. Volcanic Risks and Insurance. In *Volcanic Hazards, Risks and Disasters*, 301–314 https://doi.org/10.1016/B978-0-12-396453-3.00012-5 (Elsevier, 2015).
57. Tadini, A. et al. Uncertainty quantification in volcanology: observations, numerical modelling, and hazard/risk assessment: preface to the special issue. *Bull. Volcanol.* **87**, 48. https://doi.org/10.1007/s00445-025-01835-y (2025).
58. Marzocchi, W., Newhall, C. & Woo, G. The scientific management of volcanic crises. *J VOLCANOL GEOTH RES.* **247**, 181–189. https://doi.org/10.1016/j.jvolgeores.2012.08.016 (2012).
59. White, C. J. et al. Towards multi-hazard and multi-risk indicators–a review and recommendations for development and implementation. *NHESSD* 1–36 https://doi.org/10.5194/nhess-25-4263-2025 (2024).
60. Flanagan, B. E., Gregory, E. W., Hallisey, E. J., Heitgerd, J. L. & Lewis, B. A social vulnerability index for disaster management. *JHSEM* **8**(1) http://www.bepress.com/jhsem/vol8/iss1/3 (2011).
61. Cutter, S. L., Boruff, B. J. & Shirley, W. L. Social vulnerability to environmental hazards. In Hazards Vulnerability and Environmental Justice (115–132). https://www.jstor.org/stable/42955868. (Routledge, 2003).
62. Bindu, D. H., Siri, M. & Srivastava, N. Uncovering population patterns in volcanic areas with PCA (principal component analysis of population pattern in volcanic areas. In *2025 International Conference on Advances in Modern Age Technologies for Health and Engineering Science (AMATHE)* (pp. 1–7). IEEE.
63. Lapietra, I., García-Pereiro, T. A. & Combined Spatial Investigation of social vulnerability and flood hazard: A brief report on the metropolitan City of Bari (Southern Italy). *Spat. Demogr.* **13** (1), 8. https://doi.org/10.1007/s40980-025-00141-7 (2025).
64. Frigerio, I. et al. A GIS-based approach to identify the Spatial variability of social vulnerability to seismic hazard in Italy. *Appl. Geogr.* **74**, 12–22. https://doi.org/10.1016/j.apgeog.2016.06.014 (2016).

65. Pratschke, J. & Benassi, F. Population change and residential segregation in Italian small areas, 2011–2021: an analysis with new Spatial units. *Spat. Demogr.* **12** (2), 3. https://doi.org/10.1007/s40980-024-00124-0 (2024).
66. Lapietra, I., Colacicco, R., Rizzo, A. & Capolongo, D. Mapping social vulnerability to multi-hazard scenarios: a GIS-based approach at the census tract level. *App Sci.* **14** (11), 4503. https://doi.org/10.3390/app14114503 (2024).
67. ISTAT. Censimento Popolazione Abitazioni dataset. http://dati-censimentopopolazione.istat.it/Index.aspx
68. Tobler, W. R. A computer movie simulating urban growth in the Detroit region. *Econ. Geogr.* **46** (1), 234–240 https://www.jstor.org/stable/143141 (1970).
69. Anselin, L. & Rey, S. Properties of tests for Spatial dependence in linear regression models. *Geographical Anal.* **23** (2), 112–131. https://doi.org/10.1111/j.1538-4632.1991.tb00228.x (1991).
70. Siagian, T. H., Purhadi, P., Suhartono, S. & Ritonga, H. Social vulnerability to natural hazards in indonesia: driving factors and policy implications. *Nat. Hazards.* **70** (2), 1603–1617. https://doi.org/10.1007/s11069-013-0888-3 (2014).

Acknowledgements
This research was conducted within the RETURN Extended Partnership project and received funding from the European Union Next-GenerationEU (National Recovery and Resilience Plan—NRRP, Mission 4, Component 2, Investment 1.3—D.D. 1243 August 2, 2022, PE0000005).

Author contributions
I.L.: Writing—original draft, Software, Investigation, Formal analysis, Data curation, Conceptualization. F. B.: Writing—review & editing, Data curation. T. G-P: Writing—review & editing, Data curation. A. P.: Writing—review & editing, Data curation. P. D.: Writing—review & editing, Supervision, Funding acquisition.

Funding
This research was conducted within the RETURN Extended Partnership project and received funding from the European Union Next-GenerationEU (National Recovery and Resilience Plan—NRRP, Mission 4, Component 2, Investment 1.3—D.D. 1243 August 2, 2022, PE0000005).

Declarations

Competing interests
The authors declare no competing interests.

Additional information
Supplementary Information The online version contains supplementary material available at https://doi.org/10.1038/s41598-026-40589-1.

Correspondence and requests for materials should be addressed to I.L.

Reprints and permissions information is available at www.nature.com/reprints.

Publisher's note Springer Nature remains neutral with regard to jurisdictional claims in published maps and institutional affiliations.